A Dual-FRET-Based Versatile Prodrug for Real-Time Drug Release Monitoring and In Situ Therapeutic Efficacy Evaluation

*Shi-Ying Li, Li-Han Liu, Lei Rong, Wen-Xiu Qiu, Hui-Zhen Jia, Bin Li, Fei Li, and Xian-Zheng Zhang**

A dual-Förster resonance energy transfer (FRET)-based versatile prodrug (V-prodrug), in which the fluorescence of both 5(6)-carboxylfluorescein (FAM) and doxorubicin (DOX) can be quenched by 4-(dimethylaminoazo)benzene-4-carboxylic acid (Dabcyl) with high quenching efficiency, is developed in this paper. The V-prodrug can selectively bind to the $\alpha_v\beta_3$ integrin overexpressed cancer cells through the Arg-Gly-Asp (RGD) targeting moiety. After that, the acid-mediated DOX release of the V-prodrug can be real-time monitored by the increase of the red fluorescence from DOX. Thereafter, DOX-induced cell apoptosis can also be in situ assessed by the fluorescence recovery of the FAM, due to the caspase-3-mediated Asp-Glu-Val-Asp (DEVD) peptide sequence cleavage. This novel prodrug provides a cascaded imaging of real-time drug release and subsequent cell apoptosis, which enables the in situ detection of the cancer response and the therapeutic efficacy evaluation of the prodrug.

1. Introduction

Over the past decades, prodrugs were developed as an effective approach for cancer treatment. This strategy provides great possibilities to overcome various drawbacks of drug molecules, such as poor solubility, systemic instability, and lack of cancer specificity.[1] However, owing to the variation of patients and cancer types, a prodrug curative for one patient may not suitable for the others.[2] Under this circumstance, prodrugs with capability of real-time therapeutic efficacy evaluation are of great importance for personalized drug development.

Recently, various theranostic prodrugs were exploited for combined drug release monitoring and cancer therapy.[3] These prodrugs enable us to know when, where and how the active drug molecules were delivered,[4] and even quantitatively detect the release of active drugs in a noninvasive manner.[3e] Moreover, cell apoptosis probes were also developed for the evaluation of cancer cells response to chemotherapeutic drugs through the overexpressed enzymes associated with cancer death.[5] Cell apoptosis status combined with drug release progress would reveal more detailed therapeutic information such as the optimized drug type and dosage, and facilitate the development of the personalized drugs. Thus, a versatile prodrug with both theranostic and apoptosis detect capability was of great interest in prodrug development.[6] However, this kind of prodrug was still unrealized.

Here, a dual-Förster resonance energy transfer (FRET)-based versatile prodrug FAM-GC(Mal-hyd-DOX)SDEVDSK(Dabcyl)RGD (V-prodrug) was designed. As shown in **Scheme 1**, the V-prodrug was mainly constructed with three components. A fluorescent anticancer drug doxorubicin (DOX) was introduced into the V-prodrug using acid-labile hydrazone bond combined with a potent fluorescent quencher 4-(dimethylaminoazo)benzene-4-carboxylic acid (Dabcyl) to visualize DOX releasing. And, a Dabcyl quenchable fluorophore 5(6)-carboxylfluorescein (FAM)[7] was attached to the backbone of the prodrug through a caspase-3 enzyme cleavable peptide Asp-Glu-Val-Asp (DEVD)[8] for cancer cell apoptosis evaluation. Furthermore, a widely used cancer cell targeting ligand Arg-Gly-Asp (RGD)[9] was also employed for selective cell targeting and reduced side effects. Owing to the robust quenching capability of the Dabcyl, the V-prodrug would show no fluorescence in the original state. After RGD-mediated attachment of the V-prodrug to the cancer cells, the acidic microenvironment in cancer sites and endosomes would cleave the hydrazone bond and release the DOX with the recovery of red fluorescence. After which, the DOX-induced activation of the caspase-3 would break the DEVD peptide and reveal the apoptosis status through the increase of the green FAM fluorescence.

S.-Y. Li, L.-H. Liu, L. Rong, W.-X. Qiu, H.-Z. Jia, B. Li, F. Li, Prof. X.-Z. Zhang
Key Laboratory of Biomedical Polymers of Ministry of Education and Department of Chemistry
Wuhan University
Wuhan 430072, P. R. China
E-mail: xz-zhang@whu.edu.cn

DOI: 10.1002/adfm.201503262

2. Results and Discussion

2.1. Synthesis

The V-prodrug was obtained by two steps. Briefly, the apoptosis detecting moiety, FAM-GCSDEVDSK(Dabcyl)RGD (Apo-M), was synthesized by standard solid phase synthesis[10] using Rink amide AM resin (Scheme S1, Supporting Information).

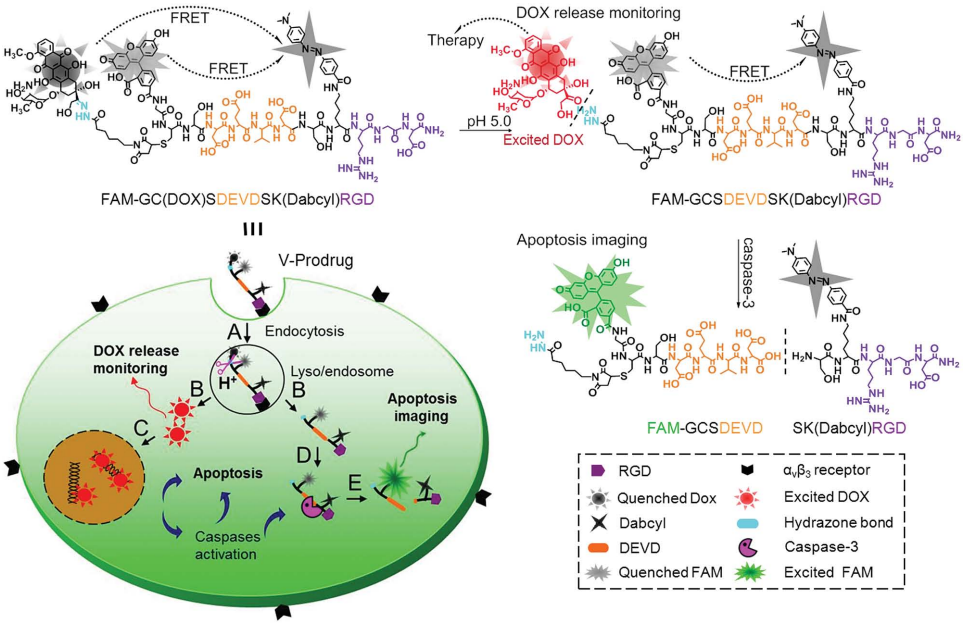

Scheme 1. Chemical structure of the V-prodrug and proposed processes of the V-prodrug for real-time drug release monitoring and caspase-3-related apoptosis imaging. Processes details: A) RGD receptor-mediated endocytosis; B) acid-mediated cleavage of the hydrazone bond and DOX release result in the emerge of the red fluorescence; C) DOX-induced cell apoptosis and caspase-3 activation; D) caspase-3-induced DEVD peptide cleavage; and E) cell apoptosis imaging through the increase of the green fluorescence (FAM).

And the V-prodrug was then obtained by attaching 6-maleimidocaproylhydrazone derivative of DOX to the Apo-M using thiol-maleimide reaction[11] (Scheme S2, Supporting Information). The structures of Apo-M and the V-prodrug were characterized (Figures S1–S7, Supporting Information).

2.2. Caspase-3 Detecting Capability

As a universal fluorescent quencher,[12] Dabcyl has been widely used in the design of molecular beacons and diagnostic probes, which can quench the fluorescence of proximity fluorophores through FRET or contact quenching process with high quenching efficiency.[13] In this paper, Dabcyl was employed as a fluorescent quencher for both FAM and DOX. First, the Apo-M was used to demonstrate the caspase-3 detecting capability of the V-prodrug. The fluorescence intensity of the Apo-M (0.5×10^{-6} M) was monitored after incubated with caspase-3 (300×10^{-12} M) in simulated physiological environment (10×10^{-3} M sodium phosphate buffer, PBS, pH 7.4; 37 °C) for different time spans. As shown in **Figure 1**a, after the addition of the caspase-3, a sustained fluorescence increase around 520 nm was observed in 7 h, showing an excellent fluorescence quenching efficiency of this FRET quenching pair (>99.2%) according to the method reported in literature.[13b] Compared to the caspase-3 presented ones, the samples without caspase-3 treatment showed negligible fluorescence change in the same condition (Figure S8, Supporting Information). The increase of the fluorescence was attributed to the addition of the caspase-3, which induced the cleavage of the DEVD/S (/ represented the cleavage site) linker and led to the separation of the FAM/Dabcyl FRET quenching pair. In addition, when the caspase-3 inhibitor Ac-DEVD-CHO[14] (50×10^{-6} M) was added to the caspase-3 (100×10^{-12} M) presented samples, no visible fluorescence change was observed (Figure 1b, magenta line), which implied the specific liability of the DEVD linker to the caspase-3. These findings suggested that the fluorescence increase observed was attributed to the caspase-3 caused cleavage of the DEVD linker in the Apo-M. Moreover, the fluorescence changes of the Apo-M in different concentrations of caspase-3 in 6 h were also investigated.

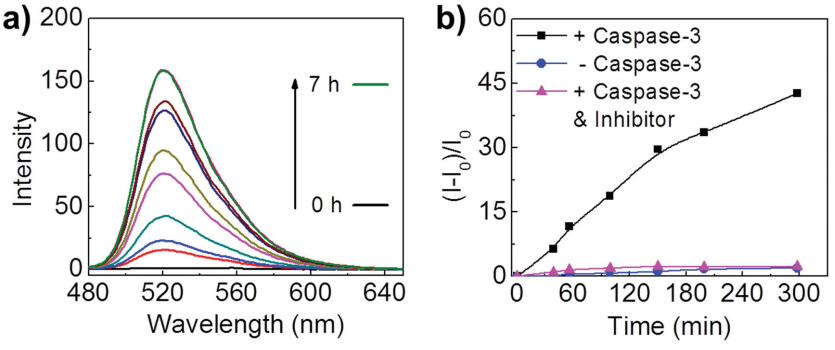

Figure 1. a) Fluorescence emission spectra of the Apo-M (0.5×10^{-6} M) incubated with caspase-3 (300×10^{-12} M) in PBS (10×10^{-3} M, pH 7.4) from 0 h to 7 h. b) Time-dependent fluorescence intensity change of the Apo-M (0.5×10^{-6} M) upon treatment with caspase-3 (100×10^{-12} M) in the presence and absence of inhibitor Ac-DEVD-CHO (50×10^{-6} M). Excitation: 465 nm; emission: 520 nm.

It was found that the fluorescence increase displayed time dependent pattern (Figure S9, Supporting Information), which was consistent with the percent of the cleavage for Apo-M input (Figure S10, Supporting Information). A linear relationship between the fluorescence intensity change at 520 nm and the caspase-3 concentration was also observed ($R^2 = 0.978$, Figure S11, Supporting Information). These data suggested that the Apo-M could be used as an efficient caspase-3 detector under biological environment.

The caspase-3 detecting capability of the Apo-M was also investigated in cellular level. Human glioblastoma cells (U87 cells) were used as cellular model. And, ultraviolet (UV) irradiation was employed as an apoptosis stimulus for the activation of the intracellular caspase-3.[15] After the addition of the Apo-M, the U87 cells were treated with UV irradiation for 1 h, and the fluorescence images were acquired using confocal laser scanning microscopy (CLSM; Nikon C1, Japan). The Apo-M treated cells without UV irradiation were used as blank control, and cells pretreated with Ac-DEVD-CHO (50×10^{-6} M) for 2 h before the Apo-M addition and the UV irradiation were used as negative control. As shown in **Figure 2**, bright green fluorescence was observed in the cells treated with UV irradiation (+ UV) while negligible green lights were found in neither blank control (Control) nor negative control (+ UV + inhibitor). To exclude the influence of the instable peptide bond caused fluorescence recovery of Apo-M under UV irradiation,[16] the fluorescence changes of Apo-M solutions under various UV irradiation times were measured in cuvettes. As illustrated in Figure S12 (Supporting Information), negligible fluorescence change was found after UV treatment, while comparable fluorescence change between Apo-M and Apo-M treated with UV irradiation was found, which verified the good stability of Apo-M under short term UV irradiation. This result was also consistent with our previous finding.[17] The green light observed was ascribed to the cleavage of the DEVD linker of the Apo-M caused by the caspase-3, which was activated by the UV irradiation. In consideration of the anticancer drug used in our V-prodrug was DOX, U87 cells were also treated with DOX (10 μg mL^{-1}) for 24 h to confirm the DOX-induced caspase-3 activation[18] could also be sensed by the Apo-M. As shown in Figure 2, similar to the UV irradiation treated samples, green fluorescence was also observed in DOX-treated cells (+ DOX) while no fluorescence was collected in cells preincubated with caspase-3 inhibitor (+ DOX + inhibitor). These results clearly showed that the Apo-M could efficiently monitor the cell apoptosis induced by DOX in cellular level. Since caspase-3 in cell might be activated in many situations, we first investigated if the released DOX in V-prodrug could induce the caspase-3 activation using western blot analysis (Figure S13, Supporting Information). Compared to the untreated U87 cells, the sensor Apo-M incubated U87 cells did not show apparent caspase-3 activation, while V-prodrug incubated U87 cells showed much high activated caspase-3 expression. Obviously, Apo-M could serve as a cell apoptosis indicator in apoptotic cancer cells. Thus, after the intracellularly caspase-3 activation-induced by released DOX from V-prodrug, the simultaneously released Apo-M could further real-time monitor the apoptotic signal in situ.

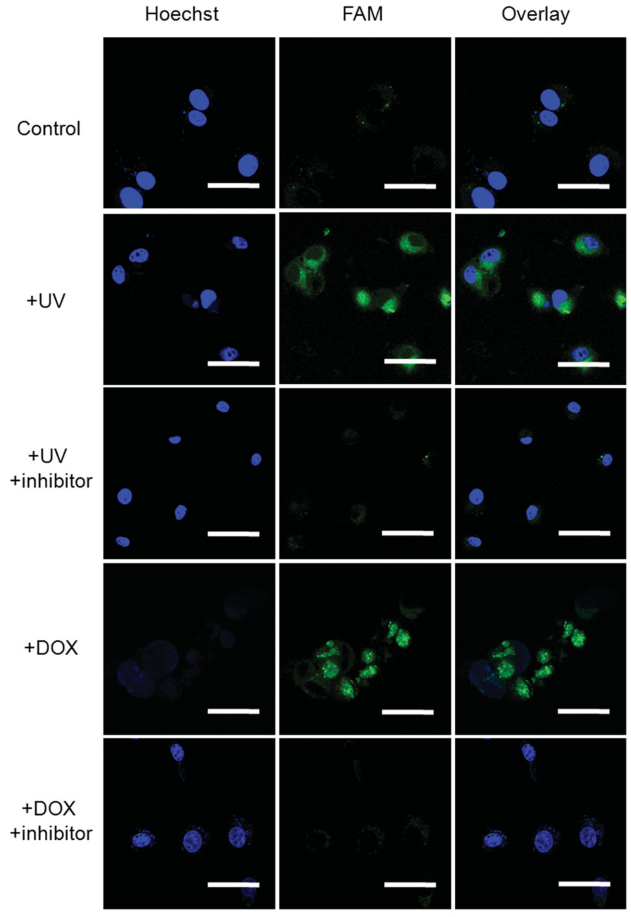

Figure 2. CLSM images of the Apo-M preincubated U87 cells (control), the Apo-M preincubated U87 cells treated with UV irradiation (+ UV + inhibitor) or DOX (in the absence and presence of Ac-DEVD-CHO, 50×10^{-6} M) (+ DOX and + DOX + inhibitor). The nuclei were stained by Hoechst 33342 labeled by blue signals. Green fluorescence: FAM. Scale bar: 20 μm.

Considering the DOX release and caspase-3 activation are long monitoring processes, a series of experiments were carried out to study if there were intramolecular FRET quenching effects between the released DOX and Apo-M, or between the released FAM and Dabcyl-peptide under physiological environment (pH 7.4). As shown in Figure S14a (Supporting Information), when different concentrations of free DOX solutions were incubated with a fixed concentration of Apo-M, the fluorescence of DOX increased linearly to its concentration. Also, when a fixed concentration of free DOX solution was incubated with gradient concentrations of Apo-M, the fluorescence of DOX at 590 nm remained untouched (Figure S15a, Supporting Information), indicating that the fluorescence of released free DOX would not be influenced by the Apo-M. Moreover, the fluorescence of DOX at 590 nm in the mixture of the DOX and Apo-M was stable within 7 h (Figure S16a, Supporting Information), suggesting that the long release monitoring process would not affect the DOX fluorescence. Similar to DOX and Apo-M, Dabcyl-peptide would not affect the fluorescence of released FAM (Figures S14b–S16b, Supporting Information). These findings strongly verified that the intramolecular FRET quenching effect could be ignored in V-prodrug, and the fluorescence changes inside cells were attributed to the DOX release and the caspase-3-induced DEVD peptide cleavage.

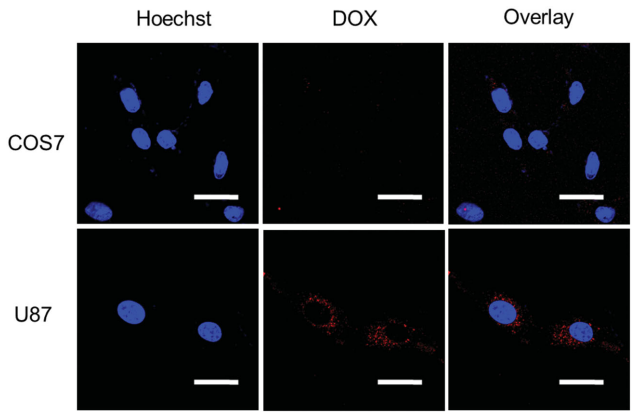

Figure 3. CLSM images of COS7 cells and U87 cells treated with V-prodrug at an equivalent DOX concentration of 10 μg mL^{-1} for 0.5 h. The cell nuclei were stained by Hoechst 33342 (blue). Red signal: released DOX. Scale bar: 20 μm.

2.3. RGD Peptide Enhanced Cancer Targeting

DOX is one of the most effective first-line antineoplastic drugs.[19] But due to its nonspecific selectivity, the excessive administration of DOX in clinic would cause acute and irreversible side effects, and lead to chronic cardiovascular diseases such as cardiomyopathy and congestive heart failure.[19,20] Thus, the cancer cell targeting property of DOX-based prodrugs was of great importance. Here, the specific targeting capability of the V-prodrug was studied in two different cell lines. A widely used $\alpha_v\beta_3$ integrin positive cell line U87 was employed as cancer cell targeting model[9b], and a $\alpha_v\beta_3$ integrin negative cell line COS7 was used as a control. The relative high expression level of $\alpha_v\beta_3$ integrin in U87 cell line than COS7 was confirmed using western blot analysis (Figure S17, Supporting Information). As shown in **Figure 3**, after incubation with the V-prodrug for 0.5 h, slight red fluorescence was found in U87 cells while no red fluorescence was observed in COS7 cells. This indicated that the V-prodrug could preferentially bind to the integrin overexpressed cancer cells. The red fluorescence in U87 cells was ascribed to the released DOX from the V-prodrug as mentioned below. The role of the RGD moiety for enhanced cancer cell uptaken was further investigated by quantitative flow cytometry analysis (Figure S18, Supporting Information). The cellular uptaken of the V-prodrug (represented in DOX fluorescence) in $\alpha_v\beta_3$ high expression U87 cell line was much higher than $\alpha_v\beta_3$ low expression COS7 cell line. Also, free RGD peptide was used to block the cellular uptake of the V-prodrug, and it was found that the cellular uptake of prodrug was noticeably decreased after the addition of RGD peptide (**Figure 4**).

2.4. Acid-Mediated Drug Release and Release Monitoring

In order to verify the acid-mediated DOX release of the prodrug, the DOX release behavior of the V-prodrug was investigated in a simulated acidic microenvironment in endosome (pH 5.0). After incubated in acetate buffer solution (ABS, pH 5.0, 37 °C), a sustained fluorescence increase around 590 nm was observed in 11 h (**Figure 5**a). This fluorescence increase was owing to the DOX released from the V-prodrug, in which the DOX fluorescence was quenched by Dabcyl with quenching efficiency of about 97%. In addition, the DOX release behavior was also investigated both in PBS (pH 7.4) and ABS (pH 5.0) through monitoring the fluorescence changes of 20×10^{-6} M V-prodrug. As shown in Figure 5b, the DOX was released at a relatively fast rate in pH 5.0 while exhibited a very slow rate in pH 7.4. In 11 h, nearly 90% of DOX were released from the V-prodrug at pH 5.0 and only about 19% of DOX were released at pH 7.4. This acid-dependent DOX release manner was attributed to the acid-labile hydrazone bond between DOX and the backbone of V-prodrug. The above results confirmed that the V-prodrug could release DOX quickly in intracellular acidic environments while remain stable in physiological conditions. Furthermore, linear relationships between cumulatively released DOX and the fluorescence intensity at 590 nm were also found in both pH 5.0 and 7.4 within 10 h (Figure 3c,d, both $R^2 > 0.995$), indicating that DOX release from the V-prodrug could be quantitatively monitored in real-time by the fluorescence intensity. Dabcyl can quench the fluorescence of the vicinal fluorephores even with low or no spectral overlap,[12,13,21] while the DOX fluorescence could be quenched through FRET process.[22] In this study, the quenching mechanism of the DOX and Dabcyl pair in V-prodrug might be the combination of FRET and contact-mediated quenching.[13]

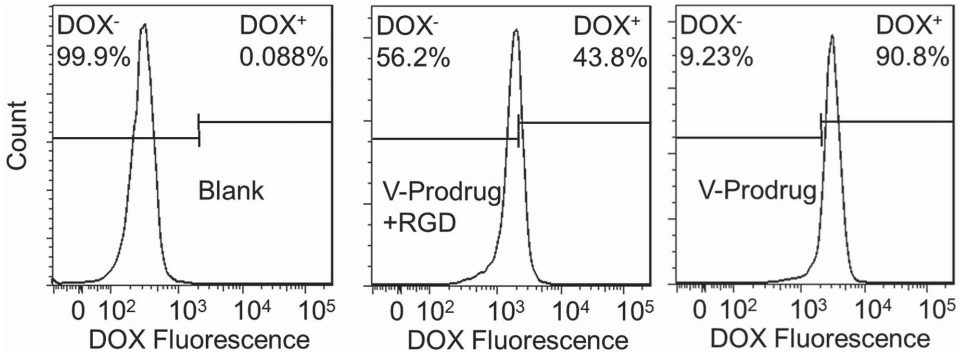

Figure 4. Flow cytometry for the quantitative analysis of cell uptake behaviors of U87 cells for V-prodrug at an equivalent DOX concentration of 10 μg mL^{-1} with/without RGD competition (0.5 mg mL^{-1}).

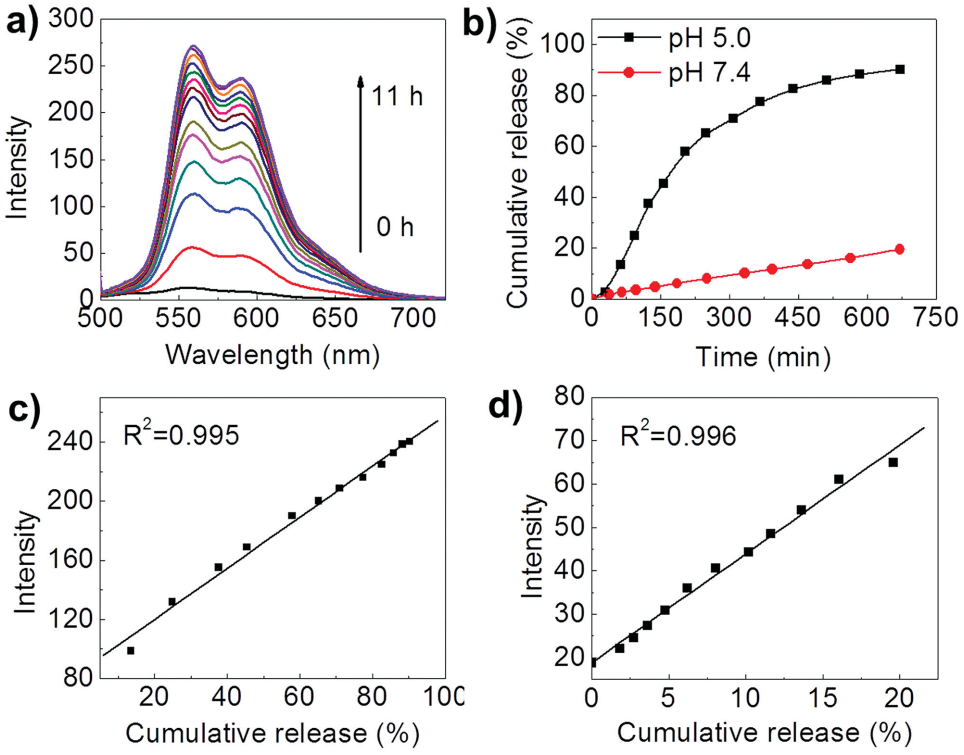

Figure 5. a) Fluorescence emission spectra of the V-prodrug (20×10^{-6} M) at pH 5.0 from 0 h to 11 h. Excitation: 488 nm. b) Cumulative DOX release from the V-prodrug as a function of time at pH 5.0 and 7.4. Excitation: 488 nm; emission: 590 nm. c) Correlation of the cumulatively released DOX from V-prodrug (20×10^{-6} M) to the recovered DOX fluorescence (at 590 nm) at pH 5.0 and d) 7.4 within 10 h.

2.5. Cellular Colocalization of the V-Prodrug

To further investigate the drug release of the V-prodrug in cancer cells, U87 cells were treated with V-prodrug at an equivalent DOX concentration of 10 μg mL^{-1} for 3 h and the acid organelles were traced by fluorescent lysosome-selective marker (Lysotracker blue, Life Technologies, USA). As shown in **Figure 6**, the fluorescence of DOX (red) showed good colocalization with the blue light (acid organelles). This colocalization implied that after integrin-mediated endocytosis of the V-prodrug, the intracellular acidic environment could lead to efficient DOX release. Meanwhile, this acid-mediated DOX release was also the reason behind the emergence of the slight red fluorescence in U87 cells in Figure 3.

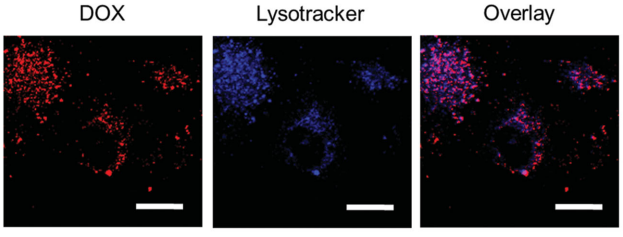

Figure 6. Subcellular colocalization CLSM images of U87 cells treated with V-prodrug at an equivalent DOX concentration of 10 μg mL^{-1} for 3 h. Blue fluorescence: Lysotracker. Red fluorescence: released DOX. Scale bar: 20 μm.

2.6. In Vitro Anticancer Activity

Cytotoxicities of the V-prodrug and the Apo-M were further investigated in U87 cells. As shown in **Figure 7**, the Apo-M displayed nearly no cytotoxicity, but the V-prodrug showed significant antiproliferative activity with a 50% inhibition concentration (IC_{50}) of 4.3×10^{-6} M. The cytotoxicity of the V-prodrug was ascribed to the DOX released in acidic environments. By the time, the probe precursor exhibited good biocompatibility, confirming that the cell toxicity was only induced by the drug DOX, which is in consistent with the result of western blot analysis above (Figure S13,

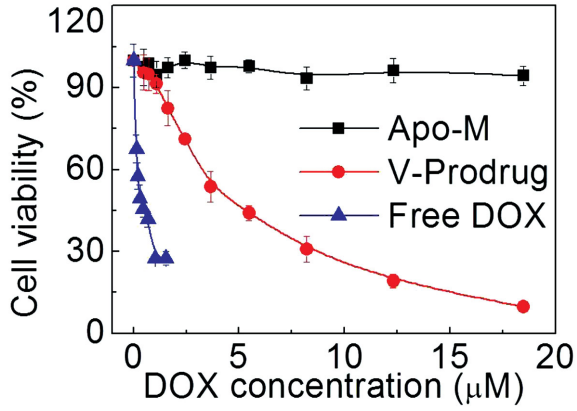

Figure 7. Cell viability of U87 cells treated with Apo-M, V-prodrug, and DOX at different DOX equivalent concentrations.

Supporting Information). Compared with free DOX (IC_{50} value of 0.14×10^{-6} M to U87 cells), the V-prodrug showed reduced cytotoxicity, this might be expected for two reasons: (i) slower endocytosis pathways of V-prodrug compared with the free diffusion of free DOX[23] and (ii) the higher cytotoxicity presented only after DOX released from the prodrug.

2.7. Theranostic Cell Imaging

Encouraged by the findings above, the V-prodrug was used for theranostic treatment of cancer cells. U87 cells and COS7 cells were treated with the V-prodrug at an equivalent DOX concentration of 10 μg mL^{-1}, and the CLSM images of the cells were acquired at different coincubation times. As shown in **Figure 8**, in U87 cells, negligible red or green fluorescence were observed after 1 h coincubation due to the excellent quenching efficiency of Dabcyl to both DOX and FAM. However, with the coincubation time increasing, both red and green fluorescence increased significantly. As demonstrated above, the red fluorescence observed was owing to the DOX released from the V-prodrug after cellular uptake. And the slow increase of the red light implied the relatively slow cellular uptake of the V-prodrug and the gradual cleavage of the hydrazone bond in it. Meanwhile, the gradually released DOX could induce the intracellular caspase-3 activation,[19] and lead to the cleavage of the DEVD linker in the V-prodrug. The break of the Dabcyl/FAM FRET quenching pair would free the FAM from its quenching state to increase the green fluorescence, indicating the activation of the caspase-3 in cancer cells. Compared with U87 cells, similar fluorescence changes were observed in COS7 cells as the prolonged incubation time (Figure S19, Supporting Information), indicating that our prodrug could realize its theranostic functions in various cell types. To further assess the cell-apoptosis imaging ability of V-prodrug, the intracellular fluorescence distributions in COS 7 cells (42 h) was visualized by *z*-stack confocal images (Figure S20, Supporting Information). Apoptotic cells exhibited apparent morphology change and strong green fluorescence while the nonapoptotic cells showed red fluorescence near the cell nuclei with ignorable green fluorescence. This phenomenon clearly demonstrated the excellent cell apoptosis discriminating ability of the V-prodrug. Based on above observations, V-prodrug was capable of drug release monitoring and released drug-induced caspase-3 activation detecting.

To further confirm the in situ caspase-3 detecting capability of the V-prodrug, U87 cells were pretreated with the caspase-3 inhibitor Ac-DEVD-CHO (50×10^{-6} M) for 2 h before coincubation with V-prodrug. As shown in **Figure 9**, after pretreated with the caspase-3 inhibitor, the increasing trend of the red fluorescence remains untouched, but no green fluorescence were observed. This disappearance of green fluorescence was attributed to addition of the caspase-3 inhibitor which blocked up the caspase-3-induced DEVD linker cleavage. This result verified that the emergence of the green fluorescence was specifically caused by the activation of intracellular caspase-3. This finding also indicated that: i) although in biological

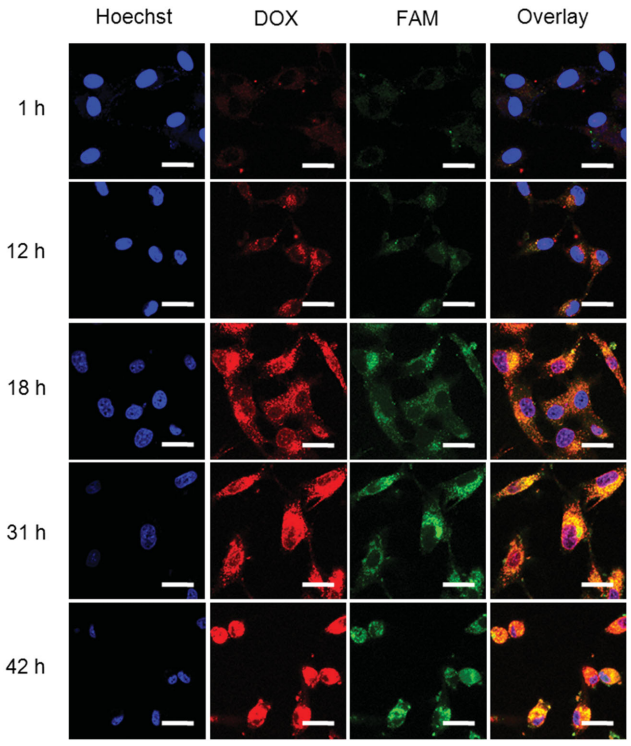

Figure 8. Time dependent confocal microscopy images of U87 cells incubated with V-prodrug at an equivalent DOX concentration of 10 μg mL^{-1} for 1, 12, 18, 31, and 42 h. The cell nuclei are stained by Hoechst 33342 (blue), the red fluorescence refers to DOX, and the green fluorescence refers to FAM. Scale bar: 20 μm.

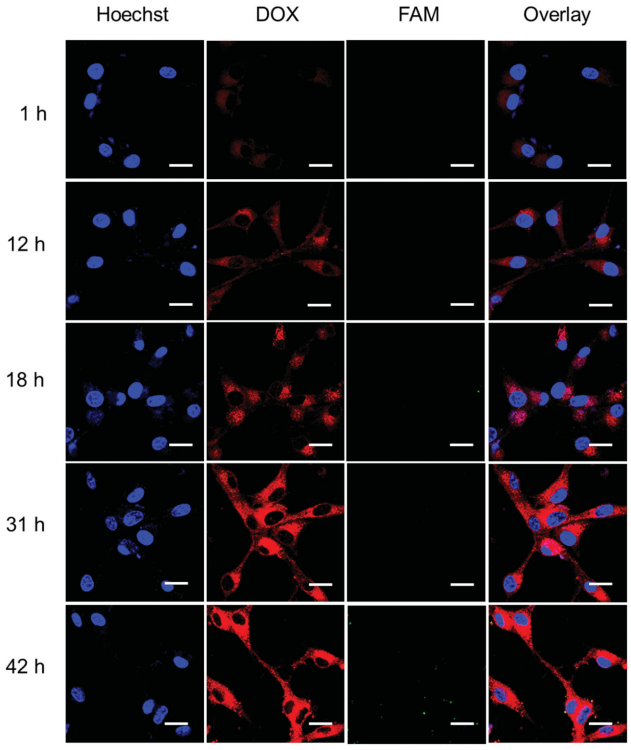

Figure 9. Time dependent CLSM images of caspase-3 inhibitor preincubated U87 cells with V-prodrug at an equivalent DOX concentration of 10 μg mL^{-1} for 1, 12, 18, 31, and 42 h. The cell nuclei are stained by Hoechst 33342 (blue), and the red fluorescence refers to DOX. Scale bar: 20 μm.

environment, the intracellular proteases might recognize and cleave the peptide into fragments and thus release DOX, but the proteases caused DOX release only contributed to a very small part of DOX release. Because the cleavage of the peptide would induce the release and fluorescence increase of FAM simultaneously, but in Figure 9, the fluorescence of FAM remained untouched in 42 h with the increasing release of DOX; ii) the DOX and carboxyl fluorescein release were sequential processes, since the blocking of activate caspase-3 significantly inhibited the FAM fluorescence recovery, the FAM release was only occurred after the DOX-release-induced caspase-3 activation.

2.8. Flow Cytometry Analysis

The flow cytometry analysis was employed to investigate cellular DOX release of the V-prodrug as well as the DOX-induced cell apoptosis in terms of the fluorescence signals (**Figure 10**). Coincided with the results in Figure 8, the percentage of DOX fluorescence positive U87 cells became increased with the prolonging coincubation time attributed to the continuous release of the DOX. At the same time, ascribed to the activation of the caspase-3 in cells by DOX, the increasing percentage of the FAM fluorescence positive cells were observed over time. In conclusion, the V-prodrug held the capability of both drug-release monitor and cell-apoptosis detection in cellular level.

3. Conclusion

In summary, we developed a novel dual-FRET-based versatile prodrug (V-prodrug) with the capability of real-time drug-release monitoring and in situ cell-apoptosis imaging. Due to the RGD moiety, the V-prodrug could selectively bind to the cancer cells and release the DOX through acid-mediated breakage of the hydrazone bond. It was demonstrated that the robust quencher Dabcyl could efficiently quench the fluorescence of DOX and FAM. This ensured the real-time DOX release monitoring and the caspase-3 imaging capabilities of the V-prodrug in cell level. In this paper, DOX was used as both a therapeutic agent and a self-reporting group for drug release. This method may pave a way for direct, precise and quantitative monitoring of the efficient DOX dose in the local site. What's more, the real-time monitor of both drug release and cell apoptosis could give the opportunity to detect the cancer response to the drugs and evaluate the therapeutic efficacy of the prodrug in situ. The therapeutic information acquired may reveal the optimized therapeutic strategies to a certain disease, and allow the emergence of the personalized drug in the near future. Noteworthy, the pharmacological profile of V-prodrug would not change much comparing to the original DOX, since the bound DOX would be transformed to the original DOX after the cleavage of hydrazone bond in acid organisms. The in vivo applications of our V-prodrug may be limited by the low tissue penetration ability of the fluorescent signal as well as background noise of tissues around visible region although good in vivo applications were found in literature using DOX and fluorophores with similar fluorescent property.[24] However, the development of in vivo imaging instruments such as dorsal skin window chamber[25] will expand their in vivo applications for therapeutic decision making and guidance of personalized cancer treatment.[25]

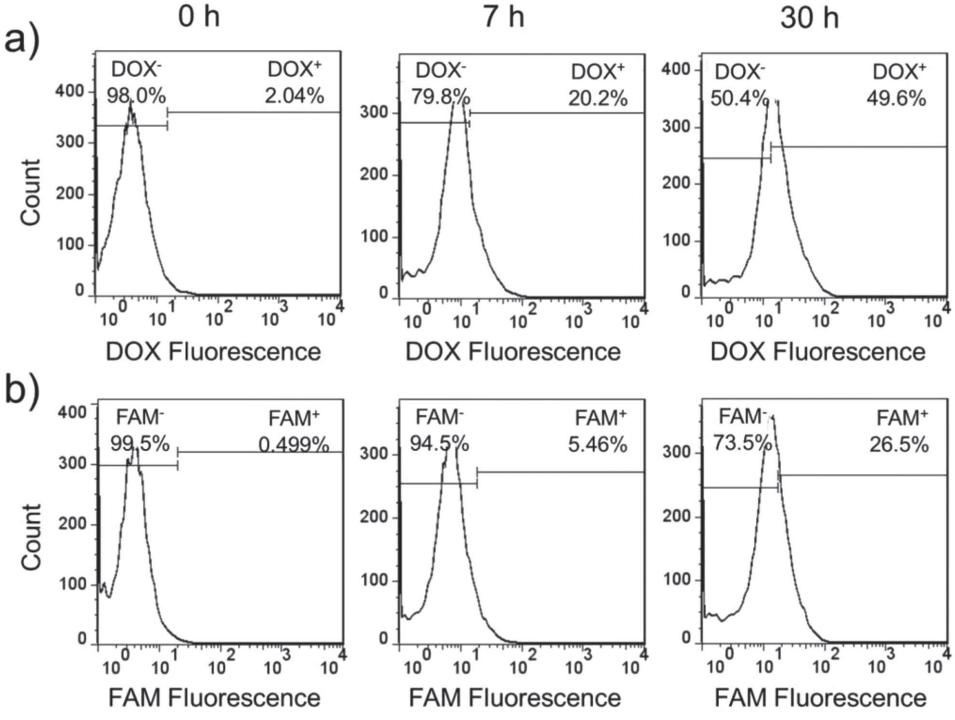

Figure 10. Quantitative flow cytometry of the a) cellular DOX fluorescence and b) FAM fluorescence in U87 cells treated with V-prodrug for 0, 7, and 30 h, separately.

4. Experimental Section

Materials: Rink amide resin (100–200 mesh, loading: 0.59 mmol g^{-1}), o-benzotriazole-*N*,*N*,*N*′,*N*′-tetramethyluroniumhexafluorophosphate (HBTU), 1-hydroxybenzotriazole (HOBt), *N*-fluorenyl-9-methoxycarbonyl (Fmoc) protected L-amino acids (Fmoc-Arg(Pbf)-OH, Fmoc-Gly-OH, Fmoc-Asp(OtBu)-OH, Fmoc-Lys(Mtt)-OH, Fmoc-Ser(tBu)-OH, Fmoc-Glu(OtBu)-OH, Fmoc-Val-OH, and Fmoc-Cys(Trt)-OH) were purchased from GL Biochem. Ltd. (Shanghai, China) and used as received. Diisopropylethylamine (DIEA) was acquired from GL Biochem. Ltd. (Shanghai, China) and used after distillation. Trifluoroacetic acid (TFA), piperidine, *N*,*N*′-dimethylformamide (DMF), phenol, acetic anhydride, methanol, dichloromethane (DCM), ethyl acetate, and anhydrous ether were obtained from Shanghai Chemical Co. (China). TFA and DMF were used after distillation. Dialysis membrane (MWCO: 1000, 2000), 6-aminocaproic acid, 2,6-lutidine, maleic anhydride, *N*-methylmorpholine (NMM), tert-butyl carbazate, thioanisole, isobutyl chloroformate, and 4-{[4-(dimethylamino)-phenyl]-azo}-benzoic acid were obtained from TCI corp. (Shanghai, China). 5(6)-carboxyfluorescein (FAM) were obtained from Aladdin Reagent Co. Ltd. (Shanghai, China). Caspase-3 (human recombinant) was purchased from Biovision Corp., and the inhibitor Ac-DEVD-CHO was purchased from Beyotime Biochem. Ltd. (Shanghai, China). Dulbecco's modified Eagle's medium (DMEM), Dulbecco's phosphate buffered saline (PBS), molecular probe (Hoechst 33342), 3-[4,5-dimethylthiazol-2-yl]-2,5-diphenyltetrazolium-bromide (MTT), and fetal bovine serum (FBS) were purchased from Invitrogen Corp. LysoTracker-Blue DND-22 was purchased from Life Technologies (USA). (6-maleimidocaproyl)hydrazone of doxorubicin (Mal-hyd-DOX) was prepared according to our previous report.[3f] All other reagents were of analytical grade and used as received.

Synthesis of Peptide FAM-GCSDEVDSKRGD: FAM-GCSDEVDSKRGD was manually synthesized by standard solid phase peptide synthesis (SPPS) using Rink amide resin and Fmoc-amino acids. The resin was first soaked in anhydrous DMF for half an hour, then the resin was treated with 20% piperidine in DMF (v/v) for 15 min twice to remove the Fmoc protecting group, after washing, the first peptide residue was coupled to the resin using 0.5 equiv. (relative to the substitution degree of resin) of Fmoc-protected amino acid (FMOC-Asp(tBu)-OH) and 3 equiv. of DIEA in a DMF solution for 3 h. Unreacted sites of the resin were then capped by a 40 min incubation with a mixture of acetic anhydride, and 2,6-lutidine in DMF (v/v/v = 5:6:89), and then the resin was treated with 20% piperidine in DMF (v/v) for 15 min twice to remove the Fmoc protecting group in the attached first amino acid, and then the rest part of peptide residues were coupled in turn by reacting with 3 equiv. of Fmoc-protected amino acid, and 3.6 equiv. of HBTU, 3.6 equiv. of HOBt, and 6 equiv. of DIEA for 2 h. After the coupling of amine acids, the resin was washed with DMF, methanol and DCM for four times, respectively, and dried under vacuum overnight. To confirm the successfully synthesize of the peptide segment Fmoc-Gly-Cys(Trt)-Ser(tBu)-Asp(OtBu)-Glu(OtBu)-Val-Asp(OtBu)-Ser(tBu)-Lys(Mtt)-Arg(Pbf)-Gly-Asp(OtBu), the peptide was cleaved from a small amount of the resin after the removing of Fmoc protecting group. Cleavage of the peptide from the resin was performed by stirring the dried resin with a mixture of TFA/thioanisole/H_2O (95:2.5:2.5) for 100 min at room temperature. The filtration was further concentrated by rotary evaporation. The residue was obtained by precipitating the viscous solution in cold ether, collected by centrifugation, and then dried under vacuum. The obtained peptide GCSDEVDSKRGD was confirmed by ^{1}H-NMR (Figure S1, Supporting Information), electrospray ionization mass spectrometry (ESI-MS), calculated MS: 1267.3, found $[M-H]^-$ = 1266.5.

Then after the removing of Fmoc protecting group, the 5(6)-Carboxyl-fluorescein (2 equiv.) was conjugated to peptide segment in rest resin using 2.4 equiv. of HBTU, 2.4 equiv. of HOBt and 6 equiv. of NMM in a DMF solution for 12 h. After the FAM-Gly-Cys(Trt)-Ser(tBu)-Asp(OtBu)-Glu(OtBu)-Val-Asp(OtBu)-Ser(tBu)-Lys(Mtt)-Arg(Pbf)-Gly-Asp(OtBu) peptide was synthesized, the resin was washed with DMF, methanol, and DCM for four times, respectively, and dried under vacuum overnight. The successfully synthesize of this peptide segment was confirmed by cleavage of the peptide from a small amount of the resin by a mixture of TFA/thioanisole/H_2O (95:2.5:2.5) for 100 min at room temperature. The obtained peptide (FAM-GCSDEVDSKRGD) was analyzed by ^{1}H-NMR (Figure S2, Supporting Information), electrospray ionization mass spectrometry (ESI-MS), calculated MS: 1624.6, found $[M-H]^-$ = 1623.5.

Synthesis of Probe Moiety FAM-GCSDEVDSK(Dabcyl)RGD (the Apo-M): The FAM-Gly-Cys(Trt)-Ser(tBu)-Asp(OtBu)-Glu(OtBu)-Val-Asp(OtBu)-Ser(tBu)- Lys(Mtt)-Arg(Pbf)-Gly-Asp(OtBu) conjugated resin was soaked in DCM for 1 h, then treated the resin with 2% TFA in DCM (v/v) for 30 min, and then 1% TFA in DCM (v/v) for 30 min to remove the Mtt protecting group, after washing the resin with DCM and DMF for four times, Dabcyl (2 equiv.) was conjugated to peptide segments using 2.4 equiv. of HBTU, 2.4 equiv. of HOBt, and 6 equiv. of NMM in a DMF solution for 12 h. After the FAM-Gly-Cys(Trt)-Ser(tBu)-Asp(OtBu)-Glu(OtBu)-Val-Asp(OtBu)-Ser(tBu)-Lys(Dabcyl)-Arg(Pbf)-Gly-Asp(OtBu) peptide was synthesized, the resin was washed with DMF, methanol, and DCM for four times, respectively, and dried under vacuum overnight. Cleavage of the peptide from the resin was performed by stirring a small amount of the dried resin with a mixture of TFA/thioanisole/H_2O (95:2.5:2.5) for 100 min at room temperature. The obtained peptide (FAM-GCSDEVDSK(Dabcyl)RGD) was confirmed by ^{1}H-NMR (Figure S3, Supporting Information), electrospray ionization mass spectrometry (ESI-MS), calculated MS: 1874.6, found $[M+H]^-$ = 1876.5. Before usage, this peptide was purified by high-performance liquid chromatography (HPLC) with a C18 reversed phase column by a linear gradient elution from 10 to 90% of acetonitrile/H_2O containing 0.1% trifluoroacetic acid at 3.0 mL min^{-1} for 20 min, the HPLC chromatogram was achieved with a UV–vis detector at 220 nm.

Synthesis of the V-Prodrug: FAM-GC(Mal-hyd-DOX)SDEVDSK(Dabcyl)RGD: Mal-hyd-DOX (1.1 equiv.), DIEA (10 equiv.), and peptide FAM-GCSDEVDSK(Dabcyl)RGD (1 equiv.) were dissolved in DMF, and stirred at room temperature for 48 h under N_2. Then the product solution was transferred to a dialysis membrane (MWCO: 2000), and dialysis against DMF for 48 h to remove the unbound Mal-hyd-DOX. The DMF solution inside the dialysis bag after dialysis was concentrated and precipitated in cold ether. The purified peptide solid was collected by centrifugation, and dried under vacuum. It was stored at a –20 °C freezer in the dark. The successful conjugation of Mal-hyd-DOX was confirmed by ^{1}H-NMR (Figure S4, Supporting Information). This peptide was purified by HPLC using the same condition with the Apo-M, and the yield of V-prodrug was 37%.

In Vitro Fluorescence Recovery Study of the Probe Apo-M: The probe was first dissolved in DMSO at 100×10^{-6} M and diluted to 1×10^{-6} M in 10×10^{-3} M pH 7.4 sodium phosphate buffer solution (DMSO/buffer = 1:99). Then the 1×10^{-6} M probe solutions were diluted to the final concentration of 0.5×10^{-6} M with buffer solutions containing recombinant human caspase-3 (0×10^{-12}, 100×10^{-12}, and 300×10^{-12} M, respectively) or buffer solution containing caspase-3 (100×10^{-12} M) and caspase-3 inhibitor Ac-DVED-CHO (50×10^{-6} M) and incubated at 37 °C. Fluorescence emission was recorded at the given time intervals with excitation wavelength at 465 nm and emission and excitation slit widths at 5 nm.

Intramolecular FRET quenching effect study.

1) Fluorescence emission study of the concentration-related Apo-M and free DOX mixture, and Dabcyl-peptide (Dabcyl-pep for short) and FAM mixture.

Apo-M at the concentration of 1×10^{-6} M was mixed with gradient concentrations (1×10^{-6}, 0.5×10^{-6}, 0.25×10^{-6} M) of free DOX, respectively. The fluorescence emission spectra of the DOX were measured by LS55 luminescence spectrometer (Perkin-Elmer) at the excitation wavelength of 488 nm.

Free DOX at the concentration of 0.5×10^{-6} M was mixed with gradient concentrations (1×10^{-6}, 0.5×10^{-6}, 0.25×10^{-6}, and 0.125×10^{-6} M) of Apo-M, respectively. The fluorescence emission spectra of the DOX were measured by LS55 luminescence spectrometer (Perkin-Elmer) with the excitation wavelength of 488 nm, and the emission wavelength were collected at 590 nm.

Dabcyl-pep at the concentration of 1×10^{-6} M was mixed with gradient concentrations (1×10^{-6}, 0.5×10^{-6}, and 0.25×10^{-6} M) of

FAM, respectively. The fluorescence emission spectra of the FAM were measured by LS55 luminescence spectrometer (Perkin-Elmer) at the excitation wavelength of 488 nm.

FAM at the concentration of 0.5×10^{-6} M was mixed with gradient concentrations (1×10^{-6}, 0.5×10^{-6}, 0.25×10^{-6}, and 0.125×10^{-6} M) of Dabcyl-pep, respectively. The fluorescence emission spectra of the FAM were measured by LS55 luminescence spectrometer (Perkin-Elmer) with the excitation wavelength of 488 nm, and the emission wavelength were collected at 520 nm.

2) Time-related fluorescence change study of Apo-M and free DOX mixture, and Dabcyl-pep and FAM mixture.

Apo-M at the concentration of 0.5×10^{-6} M was mixed with free DOX (0.5×10^{-6} M). Time-related fluorescence changes of the DOX were measured by LS55 luminescence spectrometer (Perkin-Elmer) at the excitation wavelength of 488 nm, and the emission wavelength were collected at 590 nm.

Dabcyl-pep at the concentration of 0.5×10^{-6} M was mixed with FAM (0.5×10^{-6} M). Time-related fluorescence changes of the FAM were measured by LS55 luminescence spectrometer (Perkin-Elmer) at the excitation wavelength of 488 nm, and the emission wavelength were collected at 520 nm.

In Vitro DOX Release Monitoring: The V-prodrug was dissolved in DMSO and diluted to 20×10^{-6} M in 10×10^{-3} M sodium phosphate buffer (pH 7.4) and 10×10^{-3} M acetate buffer solution (ABS, pH 5.0) (DMSO/buffer = 1:99), respectively, and then 2 mL of these V-prodrug solutions were transferred into the dialysis tubes (MWCO 1000). Immediately, the dialysis membranes were immersed in 30 mL corresponding buffer solution and incubated at 37 °C. The fluorescence of the incubation media and the original V-prodrug solution were analyzed simultaneously in the certain time intervals by LS55 luminescence spectrometer (Perkin-Elmer) at the excitation wavelength of 488 nm, emission and excitation slit widths of 5 nm.

MALDI-TOF spectroscopy of the acid treated V-prodrug (in which the hydrazone bond between DOX and peptide backbone was broken, and the DOX was released) was obtained (Figure S7, Supporting Information).

Cell Culture: COS7 cells and U87 cells were cultured in DMEM medium supplemented with 10% FBS and 1% antibiotics (penicillin–streptomycin, 10 000 U mL^{-1}) in a humidified atmosphere containing 5% CO_2.

UV- and DOX-Induced Apoptosis Imaging by CLSM: U87 cells were seeded in glass bottom dishes and incubated for 24 h. Then culture medium was replaced by probe Apo-M containing medium at the DOX concentration of 10 μg mL^{-1} at 37 °C for 0.5 h. After removing the medium and washing thrice with DMEM, U87 cells were stained with Hoechst 33342 for 15 min in the dark, and then removing the medium and washing thrice with DMEM, the cells were cultured with 1 mL of fresh DMEM containing 10% FBS in dark or exposed with UV irradiation for 1 h (power intensity: 400 μJ cm^{-2}) or treat with DOX contained medium (10 μg mL^{-1}) for 24 h, respectively. The cells images were observed by using a confocal laser scanning microscope (C1-Si, Nikon, Japan). For the control, the cells were first incubated with Ac-DEVD-CHO (caspase-3 inhibitor, 50×10^{-6} M) containing medium (1 mL) for 2 h and then replaced with probe containing medium.

Stability of the Apo-M Under UV Irradiation: Apo-M was dissolved in PBS (pH 7.4) at a concentration of 1×10^{-6} M. The fluorescence changes of Apo-M contained solutions were immediately recorded with/without 0, 10, 30, and 60 min UV treatments (power intensity: 400 μJ cm^{-2}). Excitation wavelength: 488 nm. Emission wavelength: 520 nm.

Cancer Cell Targeting Study for V-Prodrug: U87 cells and COS7 cells were seeded in glass bottom dishes and incubated for 24 h. Then, V-prodrug dispersed in DMEM medium (1 mL) with 10% FBS at the DOX concentration of 10 μg mL^{-1} were added and the cells were further incubated at 37 °C for 0.5 h. After removing the medium and then washing with DMEM (1 mL), the U87 cells and COS7 cells were stained with Hoechst 33342 for 15 min in the dark and then removing the medium and washing thrice with DMEM, then the cells were then transferred into serum containing medium (1 mL) and observed by using a confocal laser scanning microscope (C1-Si, Nikon, Japan).

Flow Cytometry for Quantitative Analysis of Cell Uptake Behaviors of COS7 Cells and U87 Cells for V-Prodrug: For the flow cytometry analysis, COS7 cells and U87 cells were seeded on 6-well plates; after 24 h incubation, the cells were incubated with the V-prodrug (at an DOX equivalent concentration of 10 μg mL^{-1}) for 15 h, and then cultured with drug free medium at pH 5.0 for 4 h to allow the breakage of hydrazone bonds in V-prodrug and the fluorescent recovery of DOX. Then, the cells were washed thrice by DMEM, and digested by trypsin, collected in centrifuge tubes, washed with PBS for three times and resuspended in 0.3 mL PBS, finally analyzed by Flow Cytometry (BD FACSAria TM III).

Flow Cytometry for Quantitative Analysis of RGD Competing Cell Uptake Behaviors of U87 Cells for V-Prodrug: For the flow cytometry analysis, U87 cells were seeded on 6-well plates, after 24 h incubation, the cells were incubated with the V-prodrug (at an DOX equivalent concentration of 10 μg mL^{-1}) or V-prodrug containing 0.5 mg mL^{-1} RGD peptide for 15 h, and then cultured with drug free medium at pH 5.0 for 4 h to allow the breakage of hydrazone bonds in V-prodrug and the fluorescent recovery of DOX. Then the cells were washed thrice by DMEM, and digested by trypsin, collected in centrifuge tubes, washed with PBS for three times and resuspended in 0.3 mL PBS, finally analyzed by Flow Cytometry (BD FACSAria TM III).

Subcellular Colocation of the V-Prodrug and Endo/Lysosome: U87 cells were seeded in a glass bottom dish and incubated in DMEM (1 mL) containing 10% FBS for 24 h. Then, V-prodrug dispersed in DMEM medium (1 mL) with 10% FBS at the DOX concentration of 10 μg mL^{-1} was added and the cells were further incubated at 37 °C for 3 h. After removing the medium and washing thrice with DMEM (1 mL), the U87 cells were stained with LysoTracker-Blue DND-22 (50 nM) for 40 min prior to imaging under a confocal laser scanning microscope (C1-Si, Nikon, Japan).

In Vitro Cytotoxicity of the Apo-M, DOX and V-Prodrug: U87 cells were seeded into a 96-well plate (5000 cells $well^{-1}$) cultured in DMEM containing 10% FBS (100 μL) incubated for 24 h (37 °C, 5% CO_2), and then DMEM (100 μL) containing a fixed concentration of the Apo-M, DOX and V-prodrug were added in each well, the cells were further incubated for 48 h at 37 °C. Then MTT solution (20 μL, 5 mg mL^{-1}) was added to each well and further incubated for 4 h. Subsequently, the MTT media were removed and DMSO (150 μL) was added to each well. The optical density (OD) was measured at 570 nm with a microplate reader (BIO-RAD 550). The relatively cell viability was calculated as follows: Viability = $(OD_{sample}/OD_{control}) \times 100\%$, where OD_{sample} was obtained from the cells treated by probe, V-prodrug, or free DOX and $OD_{control}$ was obtained from the cells without any treatments.

Real Time In Situ Drug Release Monitoring and Apoptosis Imaging: For real-time drug release monitoring by CLSM, U87 cells were seeded in a glass bottom dish and incubated in DMEM (1 mL) containing 10% FBS for 24 h. After nuclei of U87 cells were stained with Hoechst 33342 for 15 min in the dark, V-prodrug dispersed in DMEM medium (1 mL) with 10% FBS at the equivalent Dox concentration of 10 μg mL^{-1} was added. The cells images were taken by a confocal laser scanning microscope (C1-Si, Nikon, Japan) at different time intervals. The U87 cells preincubated with Ac–DEVD–CHO (caspase-3 inhibitor, 50×10^{-6} M, 2 h) were employed as the control. The confocal images of V-prodrug treated COS7 cells were taken at the same condition.

Quantitative Flow Cytometry Analysis of the Recovery of DOX and FAM Fluorescence: For the flow cytometry analysis, cells were seeded on 6-well plates and incubated for 24 h, the V-prodrug incubated U87 cells were first washed thrice by DMEM, and digested by trypsin, collected in centrifuge tubes, washed with PBS for three times and re-suspended in 0.3 mL PBS, finally analyzed by Flow Cytometry (BD FACSAria TM III).

Western Blot Analysis for Cleaved Caspase-3 Expression: After incubated with various samples (V-prodrug and Apo-M) in U87 cells for 24 h, cells were lysed with 50 μL RIPA buffer and resuspended in 50 μL 2 × SDS buffer containing 1% β-mercaptoethanol. Then the samples were heated for 5 min and separated on a 10% SDS-PAGE (15 μL per lane). After electrophoresis, proteins were transfered to a PVDF membrane (Millipore). The PVDF membranes were then blocked in PBS with 5% skim milk for 1 h. Cleaved caspase-3 was detected by incubating

the membranes with the primary antibody rabbit anti-human caspase-3 (1:2000 dilution) overnight at 4 °C and then with the secondary antibody HRP-labeled goat antirabbit IgG (1:3000 dilution, Google Biotechnology, Wuhan) for 1 h. Specific proteins were monitored by enhanced chemiluminescence. Actin was employed as protein loading control.

Western Blot Analysis for $\alpha_v\beta_3$ Integrin Expression: U87 cells and COS7 cells were lysed and treated as above. $\alpha_v\beta_3$ integrin was detected by incubating the membranes with the primary anti-$\alpha_v\beta_3$ integrin (1:500 dilution) overnight at 4 °C and then with the secondary antibody HRP-labeled goat anti-rabbit IgG (1:500 dilution, Aspen Technology) for 30 min. Specific proteins were monitored by enhanced chemiluminescence. GAPDH was employed as protein loading control.

Supporting Information

Supporting Information is available from the Wiley Online Library or from the author.

Acknowledgements

This work was supported by the National Natural Science Foundation of China (Grant Nos. 51125014, 51233003, and 21474077), the Ministry of Science and Technology of China (Grant No. 2011CB606202), and the Natural Science Foundation of Hubei Province of China (Grant No. 2013CFA003). S.Y.L. and L.H.L. contributed equally to this work.

Received: August 5, 2015
Revised: August 31, 2015
Published online: November 5, 2015

[1] a) J. Rautio, H. Kumpulainen, T. Heimbach, R. Oliyai, D. Oh, T. Järvinen, J. Savolainen, *Nat. Rev. Drug Discov.* **2008**, *7*, 225; b) I. Giang, E. L. Boland, G. M. K. Poon, *AAPS J.* **2014**, *16*, 899.
[2] M. De Palma, D. Hanahan, *Mol. Oncol.* **2012**, *6*, 111.
[3] a) S. Santra, C. Kaittanis, O. J. Santiesteban, J. M. Perez, *J. Am. Chem. Soc.* **2011**, *133*, 16680; b) S. Maiti, N. Park, J. H. Han, H. M. Jeon, J. H. Lee, S. Bhuniya, C. Kang, J. S. Kim, *J. Am. Chem. Soc.* **2013**, *135*, 4567; c) B. Kang, M. M. Afifi, L. A. Austin, M. A. El-Sayed, *ACS Nano* **2013**, *7*, 7420; d) J. P. Lai, B. P. Shah, E. Garfunkel, K. B. Lee, *ACS Nano* **2013**, *7*, 2741; e) J. N. Liu, J. W. Bu, W. B. Bu, S. J. Zhang, L. M. Pan, W. P. Fan, F. Chen, L. P. Zhou, W. J. Peng, K. L. Zhao, J. L. Du, J. L. Shi, *Angew. Chem. Int. Ed.* **2014**, *53*, 4551; f) S. Y. Li, L. H. Liu, H. Z. Jia, W. X. Qiu, L. Rong, H. Cheng, X. Z. Zhang, *Chem. Commun.* **2014**, *50*, 11852; g) S. Bhuniya, S. Maiti, E. J. Kim, H. Lee, J. L. Sessler, K. S. Hong, J. S. Kim, *Angew. Chem. Int. Ed.* **2014**, *53*, 1; h) X. M. Wu, X. R. Sun, Z. Q. Guo, J. B. Tang, Y. Q. Shen, T. D. James, H. Tian, W. H. Zhu, *J. Am. Chem. Soc.* **2014**, *136*, 3579.
[4] M. H. Lee, J. Y. Kim, J. H. Han, S. Bhuniya, J. L. Sessler, C. Kang, J. S. Kim, *J. Am. Chem. Soc.* **2012**, *134*, 12668.
[5] a) H. B. Shi, R. T. K. Kwok, J. Z. Liu, B. G. Xing, B. Z. Tang, B. Liu, *J. Am. Chem. Soc.* **2012**, *134*, 17972; b) Y. Y. Yuan, R. T. K. Kwok, B. Z. Tang, B. Liu, *J. Am. Chem. Soc.* **2014**, *136*, 2546.
[6] R. Kumar, W. S. Shin, K. Sunwoo, W. Y. Kim, S. Koo, S. Bhuniya, J. S. Kim. *Chem. Soc. Rev.* **2015**, *44*, 6670.
[7] a) J. Mu, F. Liu, M. S. Rajab, M. Shi, S. Li, C. Goh, L. Lu, Q. H. Xu, B. Liu, L. G. Ng, B. G. Xing, *Angew. Chem. Int. Ed.* **2014**, *126*, 14585; b) M. Y. Hu, L. Li, H. Wu, Y. Su, P.-Y. Yang, M. Uttamchandani, Q. H. Xu, S. Q. Yao, *J. Am. Chem. Soc.* **2011**, *133*, 12009.
[8] a) M. M. Dix, G. M. Simon, B. F. Cravatt, *Cell* **2008**, *134*, 679; b) M. Oishi, A. Tamura, T. Nakamura, Y. Nagasaki, *Adv. Funct. Mater.* **2009**, *19*, 827; c) C. Pop, G. S. Salvesen, *J. Biol. Chem.* **2009**, *284*, 21777.
[9] a) K. Welsher, Z. Liu, S. P. Sherlock, J. T. Robinson, Z. Chen, D. Daranciang, H. J. Dai, *Nat. Nanotech.* **2009**, *4*, 773; b) L. Z. He, Y. Y. Huang, H. L. Zhu, G. H. Pang, W. J. Zheng, Y. S. Wong, T. F. Chen, *Adv. Funct. Mater.* **2014**, *24*, 2754; c) L. M. Pan, J. N. Liu, Q. J. He, J. L. Shi, *Adv. Mater.* **2014**, *26*, 6742.
[10] D. Gramberg, J. A. Robinson, *Tetrahedron Lett.* **1994**, *35*, 861.
[11] C. E. Hoyle, C. N. Bowman, *Angew. Chem. Int. Ed.* **2010**, *49*, 1540.
[12] S. Tyagi, D. P. Bratu, F. R. Kramer, *Nat. Biotechnol.* **1998**, *16*, 49.
[13] a) A. M. Tang, B. Mei, W. J. Wang, W. L. Hu, F. Li, J. Zhou, Q. Yang, H. Cui, M. Wu, G. L. Liang, *Nanoscale* **2013**, *5*, 8963; b) B. Dubertret, M. Calame, A. J. Libchaber, *Nat. Biotechnol.* **2001**, *19*, 365; c) S. A. E. Marras, F. R. Kramer, S. Tyagi, *Nucleic Acids Res.* **2002**, *30*, e122.
[14] F. Li, G. Ambrosini, E. Y. Chu, J. Plescia, S. Tognin, P. C. Marchisio, D. C. Altieri, *Nature* **1998**, *396*, 580.
[15] I. K. Wang, S. Y. Lin-Shiau, J. K. Lin, *Eur. J. Cancer* **1999**, *35*, 1517.
[16] N. Huebsch, M. Gilbert, K. E. healy, *J. Biomed. Mater. Res., Part B* **2005**, *74B*, 440.
[17] S. Y. Li, L. H. Liu, H. Cheng, B. Li, W. X. Qiu, X. Z. Zhang, *Chem. Commun.* **2015**, *51*, 14520.
[18] a) K. Han, Y. Liu, W. N. Yin, S. B. Wang, Q. Xu, R. X. Zhuo, X. Z. Zhang, *Adv. Healthcare Mater.* **2014**, *3*, 1765; b) S. Kotamraju, E. A. Konorev, J. Joseph, B. Kalyanaraman, *J. Biol. Chem.* **2000**, *275*, 33585; c) A. Rebbaa, X. Zheng, P. M. Chou, B. L. Mirkin, *Oncogene* **2003**, *22*, 2805; d) S. Gamen, A. Anel, P. Lasierra, M. A. Alava, M. J. Martinez-Lorenzo, A. Piñeiro, J. Naval, *FEBS Lett.* **1997**, *417*, 360.
[19] S. Granados-Principal, J. L. Quiles, C. L. Ramirez-Tortosa, P. Sanchez-Rovira, M. Ramirez-Tortosa, *Food Chem. Toxicol.* **2010**, *48*, 1425.
[20] D. A. Gewirtz, *Biochem. Pharmacol.* **1999**, *57*, 727.
[21] J. Li, H. F. Yan, K. M. Wang, W. H. Tan, X. W. Zhou, *Anal. Chem.* **2007**, *79*, 1050.
[22] a) L. L. Lock, Z. D. Tang, D. Keith, C. Reyes, H. G. Cui, *ACS Macro Lett.* **2015**, *4*, 552; b) H. R. Krüger, I. Schütz, A. Justies, K. Licha, P. Welker, V. Haucke, M. Calderón, *J. Controlled Release* **2014**, *194*, 189.
[23] M. Prabaharan, J. J. Grailer, S. Pilla, D. A. Steeber, S. Q. Gong, *Biomaterials* **2009**, *30*, 5757.
[24] a) W. H. Chen, X. D. Xu, H. Z. Jia, Q. Lei, G. F. Luo, S. X. Cheng, R. X. Zhuo, X. Z. Zhang, *Biomaterials* **2013**, *34*, 8798; b) M. K. Yu, Y. Y. Jeong, J. Park, S. Park, J. W. Kim, J. J. Min, K. Kim, S. Jon, *Angew. Chem. Int. Ed.* **2008**, *47*, 5362; c) Y. Zhao, T. J. Ji, H. Wang, S. P. Li, Y. L. Zhao, G. J. Nie, *J. Controlled Release* **2014**, *177*, 11; d) Y. Urano, D. Asanuma, Y. Hama, Y. Koyama, T. Barrett, M. Kamiya, T. Nagano, T. Watanabe, A. Hasegawa, P. L Choyke, H. Kobayashi, *Nat. Med.* **2008**, *15*, 104.
[25] G. M. Thurber, K. S. Yang, T. Reiner, R. H. Kohler, P. Sorger, T. Mitchison, R. Weissleder, *Nat. Commun.* **2013**, *4*, 1504.